Test of a Full-Scale Steel Frame with TADAS

C. H. Yeh [1]   L. Y. Lu [2]   L. L. Chung [3]   C. S. Huang [3]

1) *National Center for Research on Earthquake Engineering, Taipei, Taiwan, R.O.C.*

2) *Department of Construction Engineering, National Kaohsiung First University of Science and Technolog, Kaohsiung, Taiwan, R.O.C.*

3) *National Center for Research on Earthquake Engineering, Taipei, Taiwan, R.O.C.*

ABSTRACT

Forced vibration tests of a full-scale bare steel frame and a frame installed with Triangular-plate Added Damping and Stiffness (TADAS) devices were conducted. This paper describes the configurations of the test frames, the instrument setup and test procedures, and the data processing and parameter identification techniques. The measured responses are processed by passing them through a band-pass filter and using a least square method to obtain frequency response functions. By modeling the test frame as a linear MDOF system, the dynamic properties, such as the modal frequencies, damping ratios and mode shapes, are subsequently identified using a nonlinear least square method. To reduce the effect of modal interference, the frequency response components from lower modes are swept out before a higher mode is identified. The inter-story stiffness of each floor is also obtained. The numerical results are discussed.

INTRODUCTION

The strength and ductility of structural systems are the most important design factors in traditional seismic designs. Recently, the development of seismic protective systems, such as base isolation and energy dissipation devices, has provided an alternative design approach for buildings and bridges [1,2]. These devices can be implemented either on the existing structures for seismic retrofitting or on new structures for vibration reduction. Although theoretical researches have shown that these devices are effective in reducing seismic responses, there are few field test data to support this assertion. Furthermore, from past experiences, it is also observed that some of the protected buildings did not perform well, and that the added devices could even cause excessive structural vibration as compared with nearby traditionally designed buildings [3]. This observation implies that some of the factors related to protection systems have not yet been identified or properly modeled. It also indicates that seismic response data of real-life structures installed with base-isolators and/or energy-dissipaters are needed for further study to increase the reliability of these devices.

To study and verify the behavior, performance, mathematical model and design procedures of various base isolation and energy dissipation devices installed on full-scale building structures, the NCREE (National Center for Research on Earthquake Engineering) in Taiwan initiated a 5-year joint research project in 1994. To fulfill the objective of the project, two identical full-scale five-story steel frames were constructed in I-lan County, Taiwan [4]. Since I-Lan County is located in one of the most seismic active zones along the northeast coast of Taiwan, it is expected that seismic response data of the test frames can be collected frequently. These steel frames equipped with accelerometers and automatic data acquisition system can provide a test bed and real-life environment for testing various seismic protective devices proposed by researchers and engineers. Figure 1 shows the map of the experimental park and the location of the two test frames.

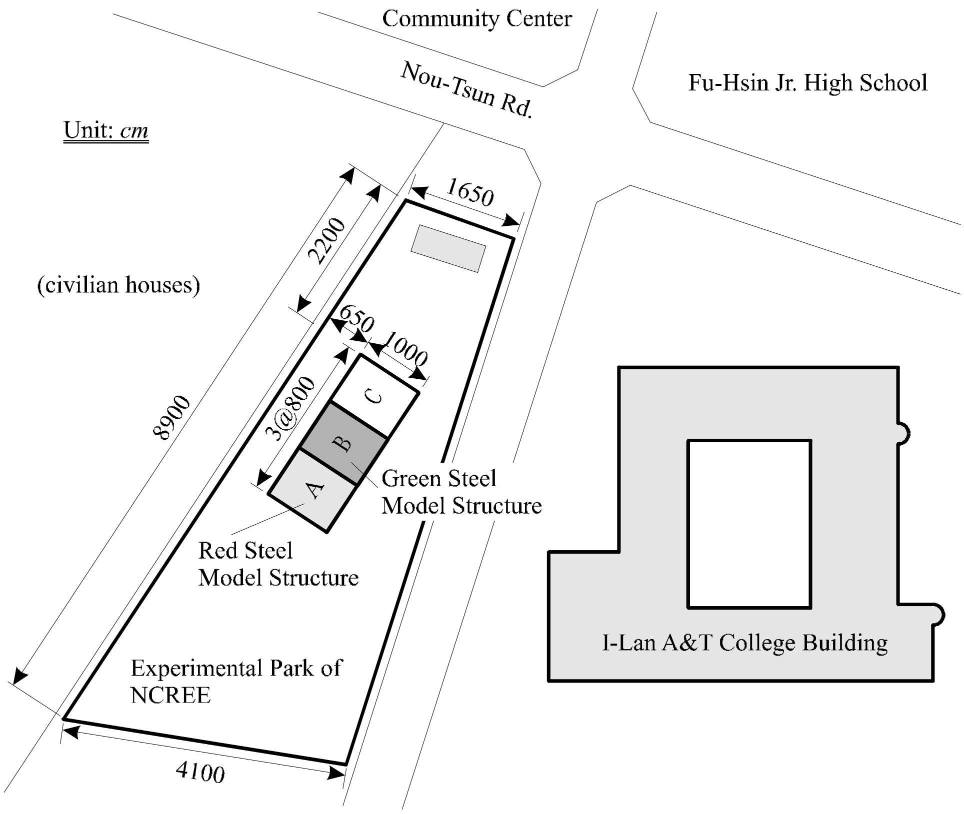

Fig. 1 Map of NCREE's I-Lan experimental park

In order to obtain the experimental modal properties of full-scale steel frames with or without the protective devices installed, a series of forced vibration tests were conducted in the project. In the literature, the forced vibration test method has been successfully applied in the measurement of the dynamic properties of large-scale structures, such as dams [5,6], nuclear power plants [7], high-rise buildings [8] and bridges [9]. In these tests, a vibration generator, located away from nodes, applied a sinusoidal force of a given frequency on the test frames. The steady-state responses of the test frames subjected to vibration at various frequencies were recorded and analyzed to obtain frequency response functions, which were further analyzed to obtain the dynamic properties of the test frame [10]. In this paper, the test procedures and results obtained from one of the two steel frames are summarized.

Theoretically, the steady-state responses of a linear system subjected to sinusoidal forces are also sinusoidal with the same frequency. However, the measured signals are always contaminated by noises, which should be eliminated or reduced [11]. The structural response near resonance is similar to that of an SDOF system, provided that the structural modal frequencies are well separated, and that the damping ratios are sufficiently small. Nonetheless, the effect of modal interference is significant in identifying a higher mode [12]. To reduce the effects of noise and modal interference, a nonlinear least square and mode-swept method is used in this paper.

PROPERTIES OF TEST MODEL

Properties of Test Frames

The test frames are full-scale, five-story steel frames, as shown in Fig. 2. To distinguish the frames from on another, one model is painted green, while the other is red (see Fig. 1). In this study, the green one was used as the test subject. The foundation is a reinforced concrete base mat 8×10×0.8 meters in dimension. Since the original soil condition was too soft, it was improved by replacing the soft soil layer with a well designed mixture of sand and gravel. As shown in Fig. 2, the depth of the improved soil layer is 2.5 meters. The floor dimension of the model is 4×6 meters (measured from center point to center point of the columns). The inter-story height is 2.6 meters (measured between the top edges of the girders). In order to simulate the dead load of each floor, eight pre-cast concrete blocks 17,300kg in total mass are mounted together on each story. The model is designed to be a soft structure. Its design yield strength is only about 80cm/sec^2.

The steel frame part of the structure is mainly composed of pre-fabricated, grade A36 W-shape beams. The dimensions of the W-shape beams are also shown in Fig. 2. At each of the four bottom corners of the steel frame, one removable short column (leg) 0.49m in height is bolted between the reinforced concrete foundation and the upper steel frame, leaving a space for future installation of base isolation devices. Also, for convenience in installing energy dissipation devices, gusset plates are added at every beam-column connection.

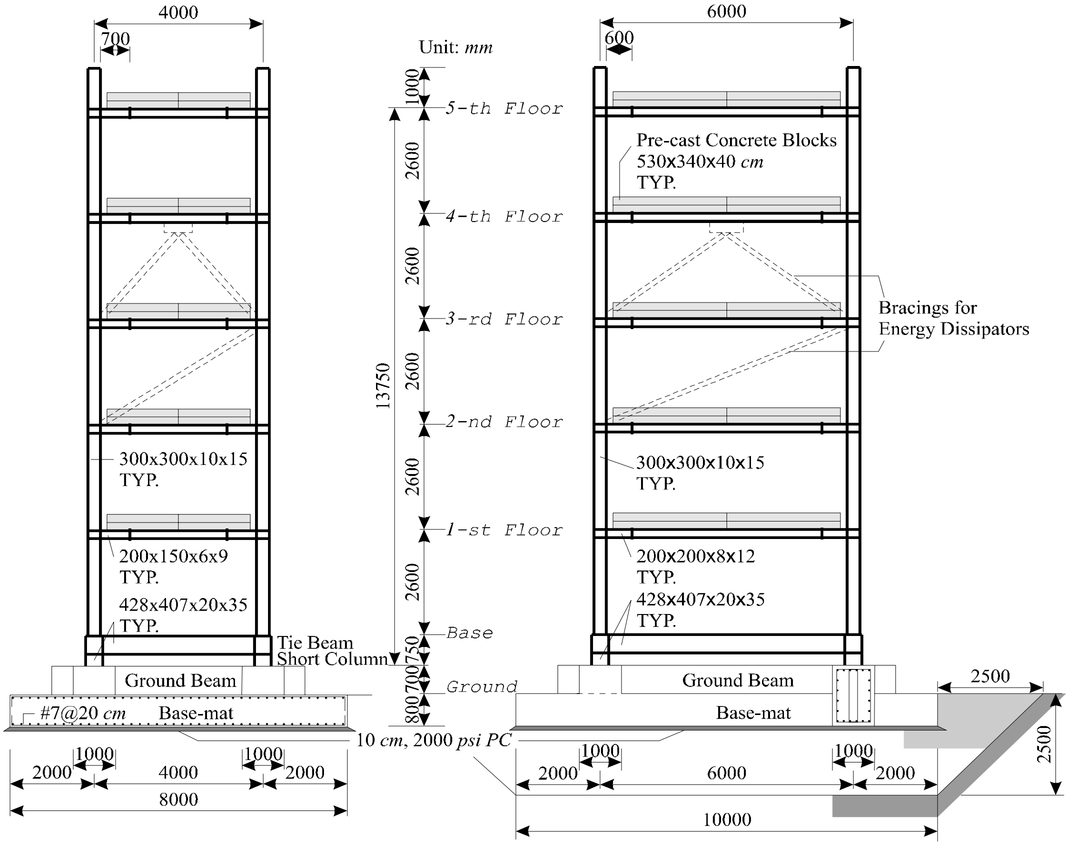

Fig. 2 Side-views of the steel test frame

Properties of Added Energy Dissipation Device

The model is tested with two different configurations, namely, a bare frame and a frame installed with energy dissipation devices. The energy dissipation device used in this study is called a Triangular-plate Added Damping And Stiffness (TADAS) device, as shown in Fig. 3. The physical dimensions and quantities of the steel plates are summarized in Table 1. For the detailed design procedures and analytic response analysis of the TADAS devices used in this test frame, readers may refer to reference [13].

Table 1 Dimensions (mm) and number of the TADAS devices used in the test frame

	TADAS in long axis				TADAS in short axis			
	Thick	Height	Base	Quantity	Thick	Height	Base	Quantity
5th Floor	16	150	100	4	16	150	100	4
4th Floor	16	150	125	4	16	150	125	4
3rd Floor	16	150	125	4	16	150	125	6
2nd Floor	16	150	150	4	16	150	150	6
1st Floor	22	150	100	4	22	150	125	6

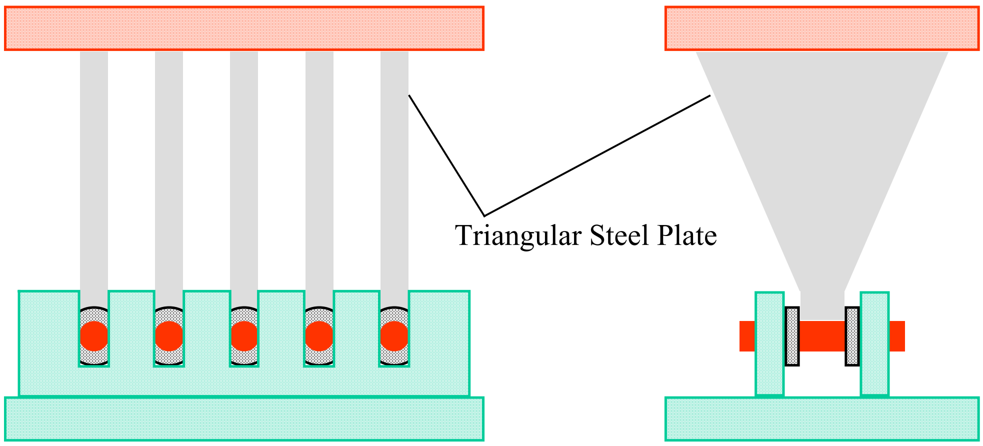

Fig. 3 Schematic diagrams of a TADAS device

A TADAS device is normally added to a frame by means of K-type bracing (see Fig. 2) and is placed at the connection of the girder and the bracing. When the device is subjected to a lateral force perpendicular to the triangular steel plates, the induced moment is linearly varied with the height of the steel plate. Since the induced moment is proportional to the moment capacity of the steel plates, the plates yield uniformly after reaching their yield capacity. This characteristic increases the energy dissipation capacity of the device. Apparently, installation of TADAS devices increases inter-story stiffness. However, the effects of hysteretic damping are significant only if the steel plates undergo plastic deformation. Since in a forced vibration test, the applied force is not large enough to cause full yielding in the steel plates, the equivalent damping ratios increase by a small amount.

EXPERIMENT SETUP AND TEST PROCEDURE

Experiment Setup

As mentioned previously, the steel frame was tested using two configurations, namely, with and without the installation of TADAS devices. Because the steel frame is symmetric about two perpendicular axes both in geometry and material properties, a Cartesian coordinate system with the origin attached to the mass center was used. The two axes X and Y were parallel with the short and long edges of the floor slab, respectively. A vibration generator system, which could generate a sinusoidal force on the test frame, was mounted on the geometric center of the roof slab (Fig. 4), implying that the excitation force was exclusively applied at the top of the steel frame. The vibration generator system was of the rotating eccentric mass type and could produce a maximum force of 42,450 Newtons at a rotary speed of 4.5Hz. In different test runs, the sinusoidal force was applied in either the X or Y direction. When the applied force was along the X-direction, a secondary moment in the Z direction, which was a sinusoidal torque with a 90-degree phase-lag behind the translational force, also occurred.

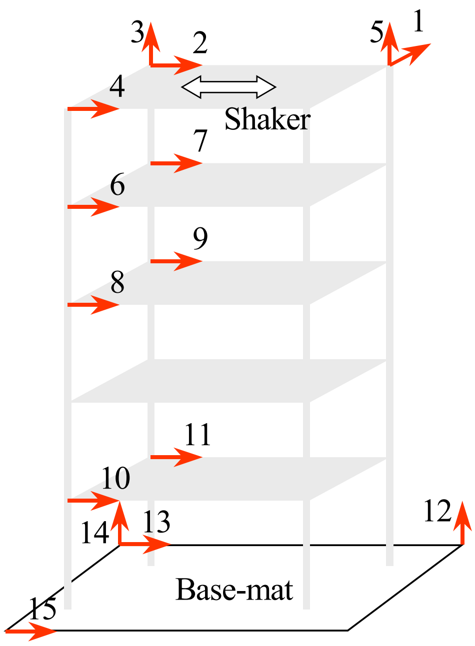

Fig. 4 Sensor arrangement and shaker location for the force vibration test

According to the structural configurations and the external force directions, the test runs were divided into four sets, labeled as GSX, GSY, GAX and GAY, respectively. The letter G stands for the green steel frame shown in Fig. 1. The letters S and A stand for the bare frame and the frame with TADAS devices, respectively. The letters X and Y stand for the external force directions.

In order to measure the dynamic response of the test frame, 15 servo-type velocity sensors and a data acquisition system were used. Figure 4 shows the locations and directions of these 15 measurements when the test sets GSX and GAX were conducted. A similar sensor arrangement was used for test sets GSY and GAY. In parallel with the direction of the applied force, two sensors were placed on each floor except for the second floor, so the translational and torsional responses of the floor slabs could be computed from these measurements. Other sensors were placed on the roof and base mat to monitor the rocking and lateral motion of the test frame.

Test Procedure

In general, the purposes of a forced vibration test are to acquire the frequency response functions of the test structure and to extract the structure's modal properties, such as the natural frequencies, damping ratios and mode shapes, from the test data. Due to the presence of a damping effect, the structural frequency response function is a complex function of the excitation frequency. The complex function is generally described by two real functions, namely, the amplitude (i.e., the absolute value of a complex number) and the phase angle. When the damping of a multistory model is small, the amplitude function will possess several spike-like peaks. Each peak signifies that one resonance frequency is found. In order to locate accurately these peaks and to record the variation of phase-lags, it is necessary to use a reasonably small frequency increment in the neighborhood of the resonance frequencies. However, a smaller frequency increment means that a larger amount of time and greater data processing effort is required in the test. Since the frequency response curves become flat between any two adjacent resonance frequencies, it is desirable to use a larger frequency increment between resonance peaks.

In order to save time and to preserve accuracy, two types of test runs were conducted, namely, a sine-sweep test and a detail test. In the former test, a larger frequency step was adopted, so rough frequency response functions covering the complete frequency range of interest were obtained in a relatively short period of time. By investigating these curves, it was possible to identify the frequency ranges in which resonance occurred. Within these ranges, detail tests, in which smaller frequency steps were used, were performed to accurately obtain the shapes of the amplitude functions and the variation of the phase functions. In this study, the frequency step was set to be either 0.2 or 0.4Hz in each sine-sweep test and 0.01, 0.02, 0.04 or 0.05Hz in each detail test, depending on the chosen frequency range. Table 2 shows the parameter settings of a typical test set, say GSX.

Table 2 Parameter settings used in test set GSX

Test Name	Test Type	Shaker Frequency (Hz)			Eccen. (kg-m)	Force (Newton)	
		f_{start}	f_{end}	Δf		Min.	Max.
GSX1	Sine Sweep	0.20	9.80	0.20	10.6	17	40200
GSX2	Detail	3.00	3.30	0.02		3770	4560
		5.30	6.20	0.02		11800	16100
		8.10	9.00	0.02/0.04		27500	33900
GSX3	Detail	0.70	1.00	0.02/0.01	21.2	410	837
		1.50	1.70	0.02/0.01		1880	1570

DATA PROCESSING AND FREQUENCY RESPONSE FUNCTIONS

It is a well-known fact that the steady-state response of a stable linear system to a sinusoidal excitation is also a sinusoidal function of time [14]. The frequency of the sinusoidal response is the same as that of the input excitation, but the phase of the response has a time lag with respect to that of the excitation. The amplitudes and phase-lags of the steady-state response can be expressed as functions of input frequencies. These functions are called the frequency response functions of the system and can be used to extract information about system characteristics, such as the natural frequencies and damping ratios of the system.

In order to obtain accurate frequency response functions of the test frame, a series of data processing techniques are used. The pulse signals, which represent the time instances when the applied force reaches maximum amplitude, are also recorded with the other velocity measurements. The frequency, f_0, and phase, ϕ_0, of the pulse signals are equivalent to the frequency and phase of the input sinusoidal force. Since the accumulated number of pulse signals (N) is linearly related to the elapsed time (t), the data points in the plot N-t should be aligned on a straight line. To reduce the effect of noise, a straight line can be obtained using a linear regression method. The frequency and phase of the pulse signals are the slope and intercept, respectively, of the straight line.

The so-called frequency response function describes the steady-state response as a function of the frequency, f, of the applied force. The steady-state response is often described by the amplitude of the response, A, and the phase lag of the response with respect to the applied force, $\Delta\phi$. Thus, in this paper, the frequency response function is plotted as a function of A versus f and $\Delta\phi$ versus f. The steady-state response at location i of the test frame can be expressed as

$$\upsilon_i(t) = C_{i0} + C_{i1}\cos 2\pi f_0 t + C_{i2}\sin 2\pi f_0 t \quad (1)$$

where C_{io}, C_{i1} and C_{i2} are constants to be determined using a linear least-square regression method. To reduce the effect of noisy signals on the identified results, the measured time series were passed through a band-pass filter before the regression was done. The bandwidth of the band-pass filter was about 1/5 that of the force frequency. Equation (1) can also be expressed in terms of amplitude, A_i, and phase, ϕ_i, that is,

$$\upsilon_i(t) = C_{i0} + A_i\cos(2\pi f_0 t - \phi_i) \quad (2)$$

$$A_i = \sqrt{C_{i1}^2 + C_{i2}^2} \quad (3)$$

$$\phi_i = \tan^{-1}(C_{i2}/C_{i1}) \quad (4)$$

At location i, the phase-lag of the response is $\Delta\phi_i = \phi_i - \phi_0$.

To make the analysis feasible, slabs of the test frame were assumed to be rigid, and only three in-plane degrees-of-freedom were considered. To measure the translation and torsion responses of each floor, there were two velocity sensors on each floor, with a distance l between them and aligned along the direction of the applied force (see Fig. 4). Because the structure is symmetrical, the translation and rotation velocities, designated by $u(t)$ and $\theta(t)$, respectively, of the mass center of a given floor slab can be computed by

$$u(t) = 0.5\,\upsilon_i(t) + 0.5\,\upsilon_j(t) \quad (5)$$

$$\theta(t) = [\upsilon_i(t) - \upsilon_j(t)]/l \quad (6)$$

where $\upsilon_i(t)$ and $\upsilon_j(t)$ are the two measurements. Since the shaker used in this study was of the rotating eccentric-mass type, the magnitude of the generated sinusoidal force was proportional to the eccentricity and the square of the rotary speed. The amplitude obtained in Eq. (3) should be divided by the magnitude of the applied force in order to obtain a normalized frequency response function.

For a linear SDOF system in steady state, the phase-lag of displacement to the applied force is between 0° and 180° while the phase-lag of displacement to velocity is 90°. As a result, in the neighborhood of the first resonance frequency, the phase-lag of velocity to the applied force should change from −90° to 90° (Fig. 5). This phenomenon can be used to check the correctness of the recorded pulse signals. However, due to modal interference in a linear MDOF system, the velocity response phase-lag will range from −180° to 180° in higher modes.

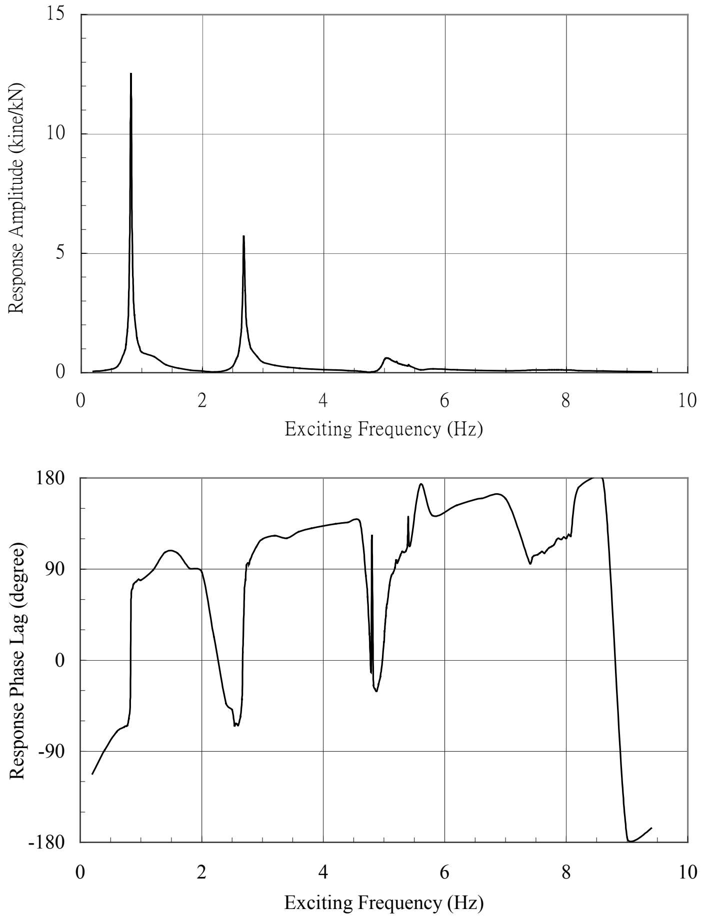

Fig. 5 Example of a frequency response function

IDENTIFICATION OF STRUCTURAL PROPERTIES

One objective of conducting a forced vibration test on a structure is to identify its dynamic properties, such as its resonance frequencies and damping ratios, from its frequency response functions. Because the recorded measurements are the structural steady-state responses, information from transient response is lost. Furthermore, since the input excitations are deterministic narrow-band sinusoidal functions, one can not obtain any useful information from a single measurement. It is for this reason that the system identification techniques involved in the forced vibration tests are almost always in frequency domain.

Modal Frequency, Damping Ratio and Mode Shape

The method of modal superposition is often used in structural dynamic analysis of a linear MDOF system. Using this method, any structural response can be decomposed into several specific modes. Each mode corresponds to a linear SDOF system with its own natural frequency and damping ratio, and any two modes are orthogonal to each other with respect to mass and stiffness matrices. In dynamic analysis, it is often sufficient to take into account only the first few modes; thus, the computational effort can be significantly reduced.

Single Degree of Freedom System

In a frequency response function, when resonance occurs, not only does the response amplitude increase a lot, but the response phase-lag also changes abruptly. By simply observing and comparing the frequency response functions of all the floors, the resonance frequencies of the first few modes can be roughly identified around the frequencies with maximum amplitudes (Figs. 6 and 7). Then, the damping ratios of these modes can be estimated using a half-power method, that is, $\varsigma \approx (f_2 - f_1) / (f_2 + f_1)$, where f_1 and f_2 correspond to the frequencies where the amplitudes drop to about $1/\sqrt{2}$ of the maximum amplitude. The mode shape can also be approximated using the amplitudes and phases of each floor slab around the peak response. Table 3 shows the identified results of the bare frame obtained using the simple observation method.

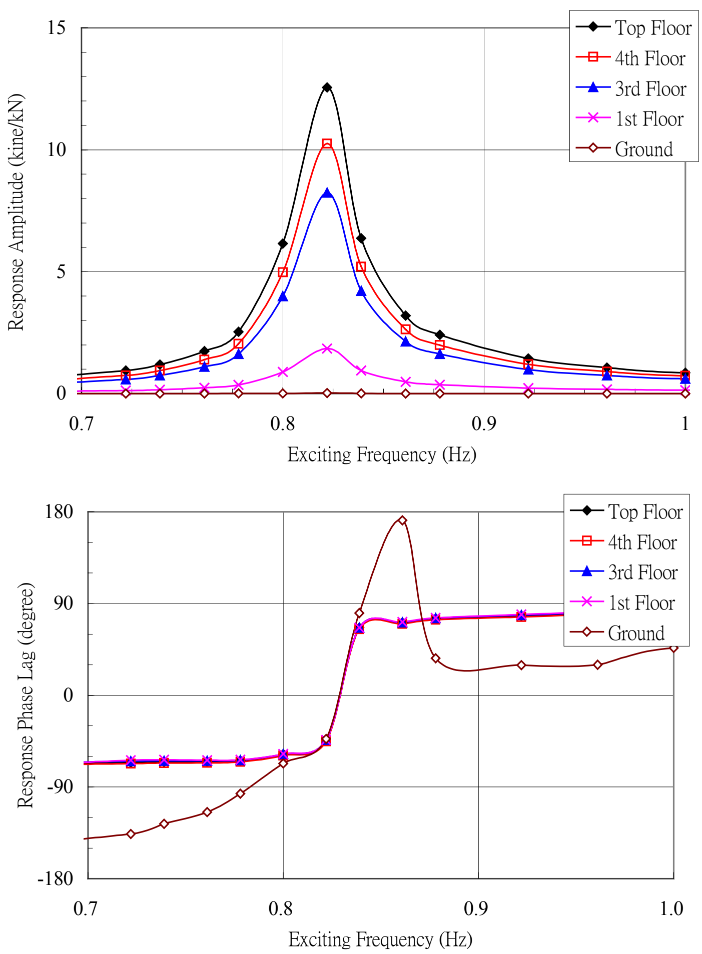

Fig. 6 Frequency response functions of translations in the Y direction in the neighborhood of the first resonance frequency in test run GSY

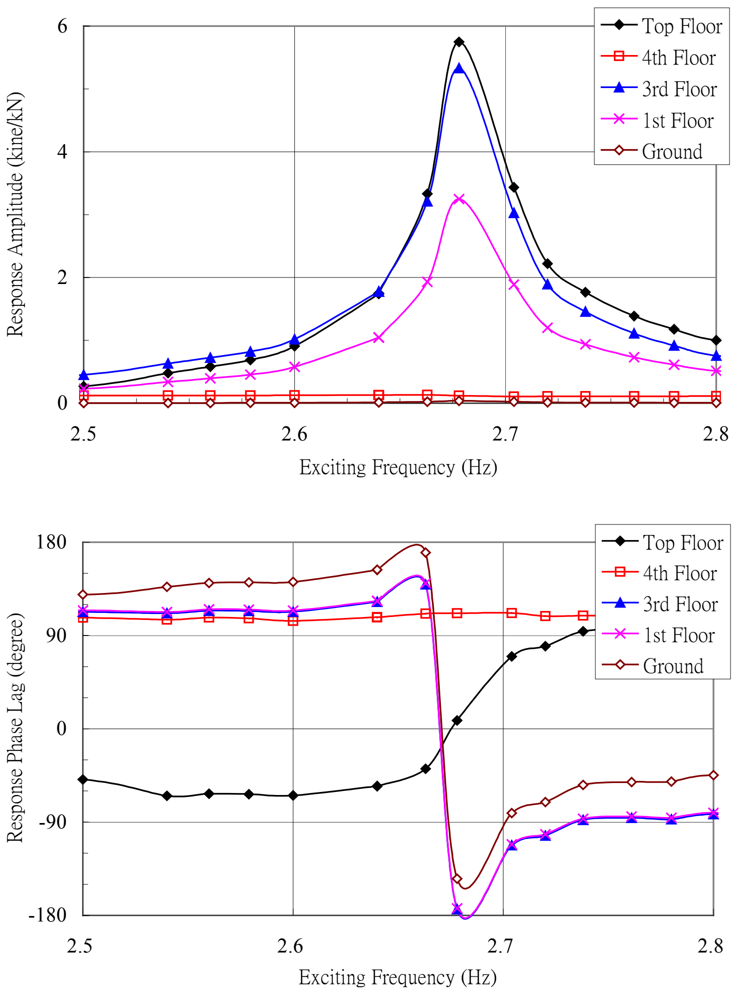

Fig. 7 Frequency response functions of translations in the Y direction in the neighborhood of the second resonance frequency in test run GSY

Table 3 Modal properties of the bare frame obtained using a simple observation method

Mode No.		1	2	3	4	5	6	7
Direction		Y	X	Z	Y	X	Y	Z
Frequency		0.82	0.89	1.57	2.68	3.18	5.01	5.50
Damping Ratio		0.014	0.009	0.005	0.006	0.012	0.016	0.007
Mode Shape	Roof	1.000	1.000	1.000	1.000	– 0.919	0.787	1.000
	4th Fl.	0.824	0.765	0.754	0.021	0.084	– 0.876	– 0.051
	3rd Fl.	0.659	0.607	0.590	– 0.929	1.000	– 0.664	– 0.915
	1st Fl.	0.148	0.131	0.130	– 0.564	0.514	1.000	– 0.541

To obtain more accurate estimations of the natural frequency, damping ratio and mode shape, consider a linear SDOF system subjected to a sinusoidal excitation; the steady-state solution of velocity amplitude, V, can be expressed as

$$V = \frac{F\,\omega}{m\,\sqrt{(\omega_1^2 - \omega^2)^2 + 4\,\varsigma_1^2\,\omega_1^2\,\omega^2}} \tag{7}$$

where m is the mass, F and ω are the amplitude and frequency of the harmonic excitation, and ς_1 and ω_1 are the damping ratio and natural frequency of the system, respectively. Taking the square of both sides and re-arranging Eq. (7), one obtains

$$\omega_1^4 V^2 + (4\varsigma_1^2 - 2)\,\omega_1^2\, V^2\,\omega^2 - (F/m)^2 \omega^2 = -\,V^2\,\omega^4 \tag{8}$$

where $\omega_1{}^4$, $(4\varsigma_1^2 - 2)\omega_1^2$ and $(F/m)^2$ are constants and can be estimated using a linear regression method [4]. The natural frequency and damping ratio can then be solved.

However, it is found that the optimal solution of Eq. (8) obtained using a linear regression method may have negative ς_1^2, which is obviously unreasonable. Hence, a nonlinear regression method can be used to obtain more accurate solutions. Table 4 shows the corresponding modal properties of the bare frame obtained using a nonlinear regression method. Since ω_1 and ς_1 can be calculated from the frequency response function of each floor, the averages of the identified values from different floors are taken as the values of ω_1 and ς_1. The mode shape is the ratio of F/m for each floor.

Table 4 Modal properties of the bare frame obtained using a nonlinear regression method

Mode		1	2	3	4	5	6	7
Direction		Y	X	Z	Y	X	Y	Z
Frequency		0.820	0.893	1.569	2.683	3.203	5.060	5.526
Damping Ratio		0.0126	0.0032	0.0039	0.0053	0.0104	0.0176	0.0072
Mode Shape	Roof	1.0000	1.0000	1.0000	1.0000	0.9459	0.9623	1.0000
	4th Fl.	0.8157	0.7673	0.7545	– 0.0698	– 0.1150	– 0.9820	– 0.0659
	3rd Fl.	0.6562	0.6078	0.5901	– 0.9228	– 1.0000	– 0.7024	– 0.8253
	1st Fl.	0.1468	0.1311	0.1296	– 0.5640	– 0.5306	1.0000	– 0.5338

Multiple Degrees of Freedom System

For a linear MDOF system, the previous method is only adequate for identification of lower modes. To identify higher modes, the effects of modal interference should be considered [12]. From modal superposition analysis of a linear MDOF system, the steady-state response of the velocity amplitude at i-th floor can be expressed as

$$V_i = \sum_{j=1}^{n} \frac{\psi_{ij}\,\psi_{5j}\,F\omega\cos(\omega t - \phi_j)}{M_j\sqrt{(\omega_j^2 - \omega^2)^2 + 4\varsigma_j^2\,\omega_j^2\,\omega^2}} \tag{9}$$

$$\tan\phi_j = \frac{2\varsigma_j\,\omega_j\,\omega}{\omega_j^2 - \omega^2} \tag{10}$$

where n is the number of modes; ψ_{ij}, M_i, ω_j and ς_j are, respectively, the i-th component of the j-th mode shape, the generalized mass, the natural frequency and the damping ratio of the j-th mode. ϕ_j is the phase-lag of the j-th mode when vibration frequency is ω. ψ_{5j} indicates that the shaker is located on the 5-th floor. After the modal properties of the first mode have been identified, the contribution from the first mode can be subtracted from the frequency response functions, and the modal properties of the second mode can be identified more accurately. By repeating the previous procedure, higher modes can be identified.

Considering the effect of modal interference, Tables 4 and 5 summarize the identified results. Comparing the dynamic parameters of the bare frame with those of the frame with TADAS devices, the modal frequency increased significantly after installation of TADAS devices. The damping ratio increased only about 2% because the responses in the forced vibration test were not large and the frames remained in elastic range. The hysteretic damping effects and the absorbed energy of the TADAS devices were significant only if the response was large enough to cause the triangular steel plates to yield.

Table 5 Modal properties of the frame installed with TADAS devices obtained using a nonlinear regression method

Mode		1	2	3	4	5
Direction		Y	X	Z	Y	X
Frequency		1.837	1.943	3.998	5.125	5.273
Damping Ratio		0.0317	0.0170	0.0256	0.0183	0.0248
Mode Shape	Roof	1.0000	1.0000	1.0000	1.0000	0.8106
	4th Fl.	0.8351	0.7632	0.7730	0.2395	0.2846
	3rd Fl.	0.6879	0.6312	0.6426	– 0.8521	– 1.0000
	1st Fl.	0.2414	0.1683	0.1723	– 0.6220	– 0.3268

Stiffness of the Structure

Tables 4 and 5 show that the damping ratios are below 3.2% for each identified mode. Due to the lack of accurate measurement of phase-lags, which significantly influence the identification results of damping ratios, the damping effect is neglected in calculating the stiffness of each floor in this study. From the equations of motion of a free vibration system, it can be found that

$$[K]\{\psi_n\} = \omega_n^2 [M]\{\psi_n\} \tag{11}$$

where $[K]$ and $[M]$ are the stiffness and mass matrices, respectively. $\{\psi_n\}$ and ω_n are the n-th mode shape and natural frequency, respectively. Assume that the mass, m_1, m_2, ... on each floor is known, and that the mass and stiffness matrices satisfy the following forms:

$$[M] = \begin{bmatrix} m_1 & 0 & 0 & \cdots \\ 0 & m_2 & 0 & \cdots \\ 0 & 0 & m_3 & \cdots \\ \cdots & \cdots & \cdots & \ddots \end{bmatrix}$$

$$[K] = \begin{bmatrix} k_1+k_2 & -k_2 & 0 & \cdots \\ -k_2 & k_2+k_3 & -k_3 & \cdots \\ 0 & -k_3 & k_3+k_4 & \cdots \\ \cdots & \cdots & \cdots & \ddots \end{bmatrix} \tag{12}$$

Substituting Eq. (12) into Eq. (11), the result is a set of algebraic linear equations. There are an equal number of unknowns and equations, so the stiffness k_1, k_2, ... in Eq. (12) can be solved for each normal mode.

If the assumptions of the lumped-mass and shear-beam type model are correct, the solutions obtained from individual modes should be identical. However, the stiffness matrix of the test frame is, in reality, a full matrix, so the numerical results of the stiffness matrix are different for different normal modes. In general, the structural stiffness is larger in the higher mode. Because there was no sensor on the second floor, the value of the mode shape on the second floor is approximated by means of interpolation. Since the variation of the curvature of the first mode shape is small, this method produces satisfactory results. If the curvature of the mode shape in the neighborhood of the second floor changes rapidly, the results will not be correct. Hence, in this study, only the first mode shape was used to identify the inter-story stiffness. The results are shown in Tables 6 and 7 with the column heading "1st Mode."

Table 6 Inter-story stiffness in the Y direction (unit: kN/mm)

	Bare Frame		Frame With TADAS Devices	
	1st Mode	Regression	1st Mode	Regression
k_5	3.03	4.61	16.96	17.08
k_4	6.22	6.73	34.14	26.63
k_3	5.31	6.03	34.33	30.41
k_2	6.05	6.86	33.05	30.66
k_1	11.89	12.83	40.90	39.24

Table 7 Inter-story stiffness in the X direction (unit: kN/mm)

	Bare Frame		Frame With TADAS Devices	
	1st Mode	Regression	1st Mode	Regression
k_5	2.84	3.02	13.21	9.27
k_4	7.18	7.22	40.92	22.10
k_3	6.42	6.52	33.36	22.55
k_2	7.38	7.53	34.82	25.56
k_1	15.04	15.29	60.17	46.13

Consider a linear MDOF system subjected to a sinusoidal excitation; the equation of motion can be expressed as

$$[M]\{\ddot{x}(t)\}+[K]\{x(t)\}=\{f\}\,e^{j\,\omega t} \tag{13}$$

where $\{f\}$ is the vector of the force amplitudes. The steady-state responses are also harmonic with the same frequency but different in phase; hence, Eq. (13) can be expressed as

$$-\omega^2\,[M]\,\{X(\omega)\}+[K]\,\{X(\omega)\}=\{F(\omega)\} \tag{14}$$

where $\{X(\omega)\}$ and $\{F(\omega)\}$ are the complex vectors of the structural responses and external forces in the frequency domain. Given a mass matrix, and input and output data and expressing the stiffness coefficients as a column vector, Eq. (14) can be expressed as

$$[X(\omega)]\,\{K\} = \{F(\omega)\} + \omega^2 [M]\,\{X(\omega)\} \qquad (15)$$

Depending on the form of the stiffness matrix, the number of unknowns can be larger than the number of equations if only one set of measurements is available. Substituting all the measurements into Eq. (15), the stiffness can be solved using linear regression method.

Following the assumptions in Eq. (12), the values of the inter-story stiffness in the X and Y directions of the bare frame and the frame with TADAS devices are summarized in Tables 6 and 7, respectively. Because similar boundary conditions and the same W-shape beams were used, k_4, k_3 and k_2 are approximately the same. However, due to the different boundary conditions of the first and the top floors, k_1 is significantly larger while k_5 is smaller than the other inter-story stiffness. Comparing the stiffness of the frame with TADAS devices with that of the bare frame, the stiffness in the Y direction increases about 420% while the stiffness in X direction increases about 350%. It is also noted that the maximum frequency of measurement is about 9Hz, so only the lower modes can be identified. To obtain higher mode properties, not only should the shaker frequency be increased, but its location also should be moved to a lower floor.

In this study, the structural stiffness matrix was also assumed to be a full matrix, but the results were not reliable. The reasons may have been as follows. First, since the measured frequency range was limited to 9Hz, only a few lower modes were covered in the test, and all the information from higher modes was lost. Second, a full stiffness matrix could be accurately identified only if all the normal modes had been measured; otherwise, the lost modes would cause the identified full stiffness matrix to lack sufficient constraints.

CONCLUSIONS

This paper has presented a systematic method for data processing and parameter identification in a forced vibration test. To reduce the effect of noises on parameter identification, the band-pass filter and linear least square method was used to calculate the frequency response functions. The modal frequencies, damping ratios and mode shapes of the test steel frame were identified using the nonlinear least square method. In order to reduce the effects of modal interference, the frequency response components of lower modes were removed before higher modes were identified. Given the mass of each floor and assuming zero damping, the inter-story stiffness of each floor could also be identified.

From the identified results, the stiffness of the frame with TADAS devices was significantly greater than that of the bare frame. However, since the frames remained in a linear elastic range during the forced vibration tests, the hysteretic damping effect on the frame with TADAS devices was not obvious.

REFERENCES

1. ATC-17-1 (1994). *Seminar on Seismic Isolation, Passive Energy Dissipation, and Active Control*, San Francisco, California, March 11~12.
2. Sakamoto, M. and Kobori, T. (1996). "Applications of structural response control — reviews from the past and

issues toward the future," *Proceedings of the 2nd International Workshop on Structural Control*, Hong Kong, Dec. 18~21.

3. Housner, G.W. and Masri, S.F. (1996). "Structural control research issues arising out of the Northridge on Kobe earthquakes," *Proceedings of the 11th World Conference on Earthquake Engineering*, Paper No. 2009, Acapulco, Mexico, June.
4. Yeh, C.H., Lu, L.Y., Chung, L.L. and Huang, C.S. (1996). "Forced vibration tests of steel frames with base-isolation and energy-dissipation devices, Part 1: bare frame and frame with TADAS," Report of National Center for Research on Earthquake Engineering, NCREE-96-003 (in Chinese).
5. Deinum, P.J., Dungar, R., Ellis, B.R., Jeary, A.P., Reed, G.A.L., Severn, R.T. (1982). "Vibration tests on Emosson Arch Dam, Switzerland," *Earthquake Engineering and Structural Dynamics*, Vol. 10, pp. 447–470.
6. Mau, S.T. and Wang, S. (1989). "Arch dam system identification using vibration test data," *Earthquake Engineering and Structural Dynamics*, Vol. 18, pp. 491–505.
7. Ibanez, P., *et. al.* (1981). "Methods and benefits of experimental structural dynamic evaluation of nuclear power plants," *Nuclear Engineering and Design*, Vol. 64, No. 1, pp. 1–32.
8. Petkovski, M., Tashkov, L. and Bom, C.S. (1992). "Full scale dynamic test of the 105-story Ryugyong Hotel in Pyongyang," *Proceedings of the Tenth World Conference on Earthquake Engineering*, Vol. 5, Madrid, Spain, July, pp. 2789–2794.
9. Salawu, O.S. and Williams, C. (1995). "Bridge assessment using forced-vibration testing," ASCE, *J. of Structural Engineering*, Vol. 121, No. 2, pp. 161–173.
10. Hudson, D.E. (1964). "Resonance testing of full-scale structures," ASCE, *J. of Engineering Mechanics Division*, Vol. 90, EM 3, pp. 1–19.
11. Muto, K., Ohta, T. and Uchida, K. (1972). "A new measuring method of vibration using correlation technique," *Proceedings of the 5-th World Conference on Earthquake Engineering*, pp. 1412–1421.
12. Hoerner, J.B. and Jennings, A.M. (1969). "Modal interference in vibration tests," *Journal of Engineering Mechanics*, ASCE, Vol. 95, No. EM4, pp. 827–839.
13. Tsai, K.C. and Yu, R.T. (1994). "Design of added damping and stiffness devices of a five-story steel test frame," Report of Earthquake Engineering Research Center of National Taiwan University, CEER-R-83-10 (in Chinese).
14. Clough, R.W. and Penzien, J., *Dynamics of Structures*, McGraw-Hill Book Co., New York (1975).